# Multimodal sub-THz radar and LiDAR imaging for NDE Applications

Vuong H. Truong, Jacob Bouchard, and Douglas T. Petkie
Department of Physics, Worcester Polytechnic Institute, Worcester, MA, 01609 USA

***Abstract*— We introduce a sub-THz FMCW radar combined with a LiDAR unit as a multimodal 3D imaging system for non-destructive evaluation applications in industry and security. A demonstration of this system is presented for a straight forward imaging scenario of targets concealed behind cardboard obscurants for manufacturing quality control. The radar imaging system operates near 100 GHz by raster scanning a confocal mirror. The 2D LiDAR sensor is mounted to the raster scanning mirror of the radar unit to capture a 3D point cloud. The LiDAR unit can serve to identify the external features that will provide parameters to optimize the radar performance and to assist in the deconvolution of the obscurant clutter from the target signatures that include image intensity, coherent detection of motion, and micro-Doppler signatures.**

## I. INTRODUCTION

THE submillimeter or terahertz (THz) spectrum has garnered interest in numerous fields, namely security, medical, and manufacturing quality assurance, of which the latter is the focus of this work. The combination of image resolution and dielectric penetrating capacity has made this spectral region attractive for non-destructive evaluation (NDE) applications. However, the signature science in the millimeter-wave/THz region for standoff imaging applications remains complex for both obscurants and targets that depends not only on the dielectric constants, but the obscurant and target orientation, geometry, surface roughness, as well as the illumination strategies, FMCW sweep, and wavelength to be able to successfully identify a target. As active millimeter-wave and THz imaging continues to expand into more complex environments, such as concealed weapon detection [1, 2], defect detection in materials [3], and identifying micro-Doppler signatures[4], additional complementary technologies can be integrated to address the complexity of the signature environment, such as visible and IR imaging, ultrasound, and LiDAR systems. Image or sensor fusion techniques can help mitigate obscurant feature and increased the probability of target identification [5].

Although optical-like image acquisition and characterization can be lengthy, there are circumstances where resolution isn't as substantial a factor, and therefore a method for a cost-effective technique in quantifying items in a manufacturing environment when packaged boxes may have insufficient items such as cans, bottles, etc., is proposed.

The incorrect assembly of products leads to millions of discarded goods daily [6]. The current quality control (QC) methods utilize random selection, weighting contents, or visual inspection which lacks obscurant penetration (surface of packages), thus a more precise method is needed. Utilizing a LiDAR's range capabilities to construct a 3D point-cloud or contour map allows the identification of targets on the assembly line. The LiDAR scans generate regions of interest (ROI) for target evaluation, and front surface obscurant details, to optimize the sub-THz radar modality, the bandwidth (BW) of the FMCW sweep in this particular case. This multimodal inspection will maximize the signal-to-noise of the target to clutter thus improving the image quality and efficiency of NDE inspection of obscured targets.

With the 2D LiDAR system (TiM781-2174101, SICK, Inc., Minneapolis, MN) mounted on top of a 12-inch diameter, 1 meter focal-length mirror, a 3D LiDAR point-cloud data are collected through the mirror's vertical sweep of the 2D scans. The LiDAR's horizontal & vertical angular resolution is 0.33 degrees, that constructs a 2D matrix of ranges. The matrix is analyzed for potential targets, who's coordinates are transformed and transferred to a centralized control system synchronized with servo motors of the mirror. The coordinate transformation directs the THz single-pixel raster scanning on the target of interest. Range data is further utilized to optimize the range resolution ($\Delta r = c/2 \cdot BW$) of the radar system.

To improve the S/N ratio, the transmitter is amplitude modulated at 50.0 kHz and the linear FMCW sweep, centered at ~96 GHz is swept at 1.0 kHz and a lock-in amplifier is used for I/Q coherent detection at a particular harmonic number associated with a target in a particular range bin. The sub-THz radar is similar to that of the 120 GHz Frequency Shift Keying (FSK) Radar System in Petkie, *et. al* [7], with the exception that a linear FMCW sweep over a bandwidth and harmonic lock-in I/Q detection is utilized in place of the FSK method. The transmitter/receiver are co-propagated to the 12-inch diameter, 1-meter focal length mirror to obtain an illuminating spot width of ~2 cm in the plane of the target. The objects used for imaging are strategically chosen to possess flat metallic surfaces and oriented normal to the mirror to enhance spectral reflection and minimize diffuse reflections. In addition, representing the scenario of detecting packaged cans on a manufacturing line.

The obscurant for this work is a flat cardboard sheet, with two 6.5 cm diameter aluminum cans placed opposite to the active system, 2.55 m from center of mirror, and total optical path length of 3.65 m. With the contour of the cardboard target extracted from the LiDAR, a pattern recognition algorithm is than utilize to find the "box". The coordinates of the box are then transferred to the THz imaging system for further

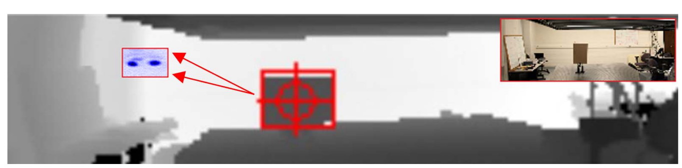

**Fig. 1.** LiDAR contour scan of the optical table and room. The red crosshair signifies the pattern recognition algorithm located the target to record a sub-THz reflected intensity image shown in the inset (left) that identifies two targets. The grey scale of the LiDAR image is proportional to distance and the dark blue indicated two strongly reflecting targets. Right inset is an optical comparison from the vantage point of the LiDAR.

evaluation, in this case, quantification of the contents of a box.

## II. RESULTS

The entirety of this work, including the centralized control system was program in LabView. This includes the LiDAR's point-cloud data extraction, target recognition algorithm, THz modulation and imaging, and finally can counting. The LiDAR is set by default to execute a vertical scan of ~36º with a horizontal range of 90 º (Fig. 1) coupled to the vertical sweep of the mirror. This, along with the algorithm takes ~7 seconds including the coordinate transformation and optimization of the range binning (frequency bandwidth) on the signal generator (Agilent E5482A). An additional 2 minutes is than needed for THz imaging by raster scanning the generated ROI (Fig. 2).

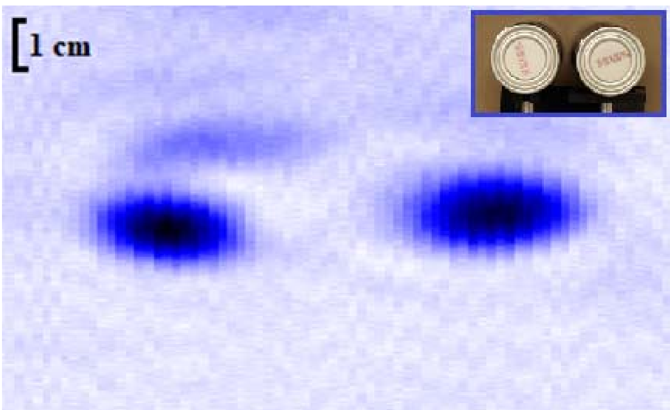


**Fig. 2.** Raster-scan THz Image of two 6.5 cm diameter aluminum cans obscured behind cardboard acquired in 130 secs. Inset is an optical image for

Optical-like resolution wasn't a factor in this work, but timing and SNR was, for which the LiDAR's contour data not only give us the ROI but in addition, the range of the target to enable BW modulation for optimal resolution. To validify the LiDAR's range determining capabilities for range bin optimization, a flat annular oscillator with 10 cm diameter oscillating at 4 Hz was position in between the cans & mirror, and the system was modified into a Michelson interferometer in order to collect phase information. The oscillator was positioned 1.75 m from the mirror, giving a 1-way optical path length of 2.85 m. Due to Fresnel diffraction from the surface of the mirror, the 2nd range bin was preferred for data acquisition. At that range, the LiDAR's suggested BW would be 105.26 MHz. A test was run with bandwidth modulation at 108 MHz in addition to amplitude modulation. The target was confirmed to be in the center of the 2nd range bin with the double peak pattern observed (Fig. 3), in agreement with the LiDAR's suggested bandwidth.

## III. SUMMARY

The initial study utilizing a LiDAR for contour mapping with machine vision has demonstrated the advantage of creating an ROI for efficient THz non-destructive imaging along with optimizing the image contrast and can mitigate the cluttered environment for subsurface sensing. The integrated system effectively count the number of obscured cans with a relatively short dwell time. Future work will examine how the FMCW radar range bins can be optimized with I/Q detection techniques to mitigate the cluttered environment due to front surface

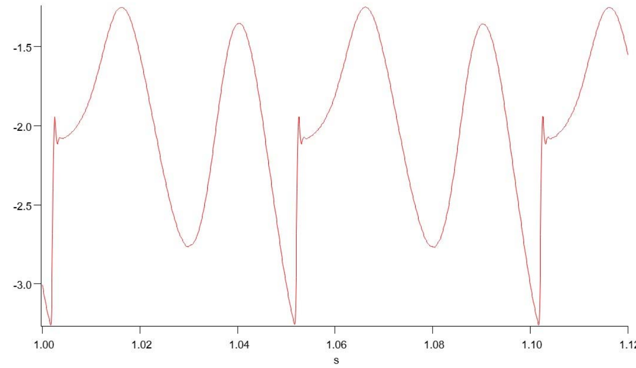


**Fig. 3.** Amplitude modulation with a bandwidth of 108 MHz, giving a range resolution of 2.78 meters in the 2nd range bin. The repeated double-peak pattern observed corresponds to a peak in that bin.

reflections of the obscurant. Machine learning algorithms for known target signatures can be developed to improve target identification for the manufacturing lines and assist in the identification of targets in an increasing complex environment such as concealed weapon detection [2]. Additionally, the system in its current form possess the capabilities to be mobile, enabling evaluation on a real assembly line. Further studies in angular diversity and how it affects the dynamic range can improve the illumination, along with continuing testing of different dielectric media since mismatches were observed, causing a 5% reflection coefficient [8], adding up to ~10% for two-way transmission. Logarithmic signal processing may be implemented to saturate the target signature. Some issues can be resolve by utilizing linear servo motors, as oppose to a gimbal mount where the angular orientation and therefore the optical path length is varied, leading to coherent effects. In an assembly line, we expect these limitations to be lifted.

## REFERENCES

[1]. D. M. Sheen, D. L. McMakin and T. E. Hall, "Active millimeter-wave and sub-millimeter-wave imaging for security applications," 2011 International Conference on Infrared, Millimeter, and Terahertz Waves, pp. 1-3, 2011.

[2]. S. R. Murrill, C. C. Franck, E. L. Jacobs, D. T. Petkie, and F. C. De Lucia, "Enhanced MMW and SMMW/THz imaging system performance prediction and analysis tool for concealed weapon detection and pilotage obstacle avoidance," Applied Optics 56 (3), B231, 2017.

[3]. D. T. Petkie, I. V. Kemp, C. Benton, C. Boyer, L. Owens, J. A. Deibel, C. D. Stoik, M. J. Bohn, "Nondestructive terahertz imaging for aerospace applications," Proc. SPIE 7485, Millimetre Wave and Terahertz Sensors and Technology II, 74850D; doi: 10.1117/12.830540, 2009.

[4]. Y. Balal, N. Balal, Y. Richter, Y. Pinhasi, "Time-Frequency Spectral Signature of Limb Movements and Height Estimation Using Micro-Doppler Millimeter-Wave Radar," Sensors 2020, 20, 4660; doi:10.3390/s20174660

[5]. E. Blasch, Z. Liu, D. T. Petkie, R. Ewing, F. Pomrenke, and K. Reinhardt, "Image fusion of the Terahertz-visual NAECON Grand Challenge data," National Aerospace and Electronics Conference, Proceedings of the IEEE. 220-227. 10.1109/ NAECON.2012.6531058, 2012.

[6]. Cook, T. M. (2016, July 22). 6 million cans a day fly off the lines at Ball Corp.'s plant in Golden. *The Denver Post*.

[7]. D. T. Petkie, E. Bryan, C. Benton, C. Phelps, J. Yoakum, M. Rogers, and A. Reed "Remote respiration and heart rate monitoring with millimeter-wave/terahertz radars", Proc. SPIE 7117, Millimetre Wave and Terahertz Sensors and Technology, 71170I; koi:/10.1117/12.800356, 2008.

[8]. D. T. Petkie, C. Casto, F. C. De Lucia, S. R. Murrill, B. Redman, R. L. Espinola, C. C. Franck, E. L. Jacobs, S. T. Griffin, C. E. Halford, J. Reynolds, S. O'Brien, and D. Tofsted, "Active and passive imaging in the THz spectral region: phenomenology, dynamic range, modes, and illumination," Journal of the Optical Society of America B-Optical Physics, 25(9), 1523-1531, 2008.

[9] TiM$10k Challenge, SICK. https://www.sick.com/us/en/tim10k/w/tim10k/